

## T. A. McMahon

Division of Applied Sciences  
Harvard University  
Cambridge, Massachusetts 02138

# Mechanics of Locomotion

## Abstract

*Energetic and mechanical principles of walking and running are reviewed, using information available from force-plate studies. A mathematical model of walking is described that conserves the sum of the kinetic and gravitational potential energies of the body. In running, energy is stored transiently in the elastic deformations of stretched muscles and tendons. Theory and experiments are described using these principles and others to find the range of stiffness values for a running track that both lowers the potential for injuries and increases running speed.*

## 1. Introduction

In bipeds, walking and running can be distinguished from a mechanical point of view on the basis of a simple test. In running, but not in walking, there is a period when both feet leave the ground. The equipment carried by Marey's (1874) runner (Fig. 1) is designed to record the time each foot is on the ground. For good measure, the runner also carries an accelerometer on his head.

The accelerometer looks like an afterthought, but it turns out to be an idea ahead of its time. An accelerometer located at the center of mass of the body would allow measurement of the mechanical work done on the (assumed solid) body during activity, provided the mass of the body were known.

The goal of this paper is to convey an appreciation of the extent to which the laws of physics are important in walking and running. A central question will be

how energy is stored and transformed as the limbs move. Insights based on the mechanics of running will pay a certain dividend—at the end of the paper we will see how these facts and some other engineering principles may be used to design a running track on which faster speeds are possible than on any other surface. But first it will be necessary to establish some basic ideas about the dynamics and energetics of walking and running, and this brings us back to measurements concerning accelerations of the center of mass.

## 2. Force Plates

A better instrument than Marey's headpiece for determining the acceleration of the center of mass is a force plate. This is a sensitive electronic scale that measures not only the vertical force but also the horizontal and lateral forces applied to it by the subject's foot.

There are three criteria for good performance of a force plate. First, the frequency response must be satisfactory, which generally means that the natural frequency of the plate (when the subject is standing on it) must be high enough, typically above 200 Hz, to follow rapid changes in the applied force. Second, the plate must give the same signal for a given force, irrespective of where that force is applied (at the center of the plate, or at an edge). Third, there must be an acceptably low level of cross-talk—spurious signals coming through one channel (for example, the one measuring vertical force), when a force is applied purely to one of the other channels (horizontally or laterally). A high-performance force plate is typically a lightweight, rigid platform suspended on a suitable arrangement of force transducers, which may be piezoelectric crystals or stiff spring elements instrumented with strain gauges.

When high-speed motion pictures are taken of a subject moving over a force plate, a great deal of mechanical information can be obtained about the gait, including the forces and moments about the various joints as well as the trajectories of those joints, and therefore the potential and kinetic energies of each of

---

With the exception of a few modifications, this paper is excerpted from *Muscles, Reflexes and Locomotion*. © 1984 by Thomas A. McMahon. Reprinted by permission of the author and Princeton University Press.

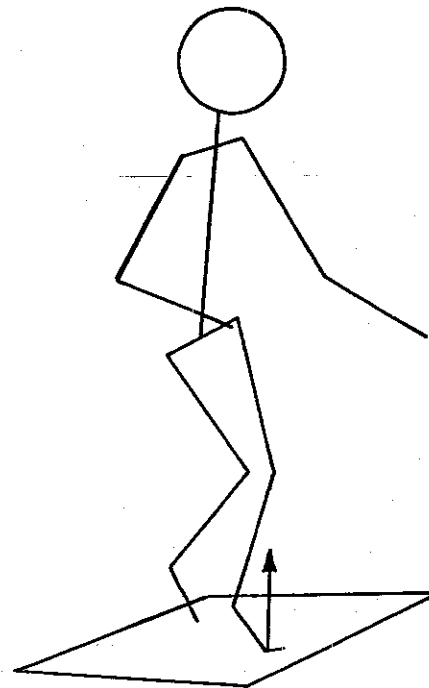
The International Journal of Robotics Research,  
Vol. 3, No. 2, Summer 1984,  
0278-3649/84/020004-25 \$05 00/0,  
© 1984 Thomas A. McMahon, Princeton University Press.  
Reprinted by permission of the copyright holder and  
Princeton University Press

Fig 1 Runner carrying a clockwork recorder for making records of walking and running. Air chambers in the shoes communicate with the recorder via rubber tubes



The device on the runner's head is an accelerometer, and he holds in his left hand a bulb for starting the pen recorder (From Marey 1874)

Fig 2. Schematic representation of a subject walking over a force plate (rectangle). The arrow shows the direction and magnitude of the ground-reaction force



the limb segments. Figure 2 shows a schematic stick figure as it might be drawn in an oblique view from information obtained from lateral and frontal film records. The magnitude and direction of the ground-reaction force measured by the force plate under the subject's foot is also shown.

### 3. Force-Plate Records of Walking and Running

Perhaps it may seem that the net effect of using a force plate is to make the analysis of walking and running more complicated. Nothing could be further from the truth. There is a simple conclusion available from force-plate records of both walking and running, as we shall see.

In Fig. 3, the vertical force has been used to provide a calculated record of changes in the mechanical energy of the body's center of mass. One integration of the horizontal force divided by mass gives changes in the forward speed of the center of mass; these have

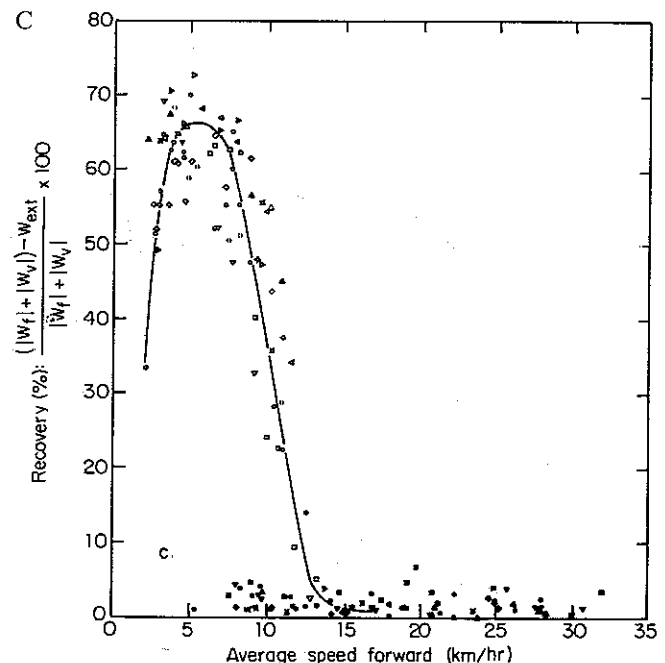
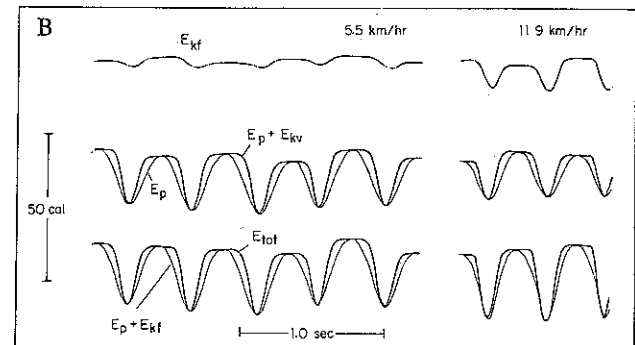
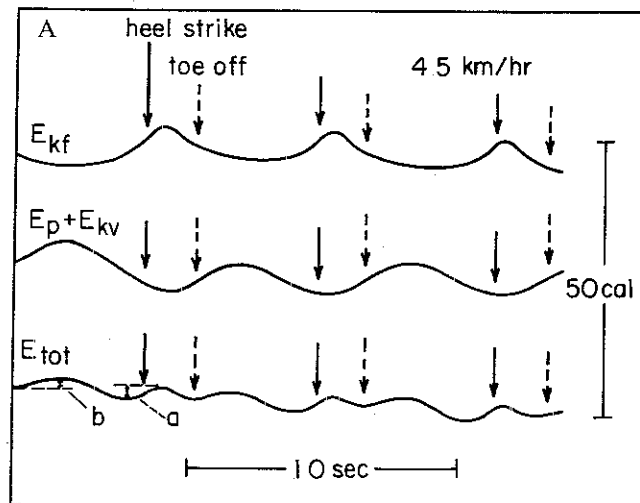
been used to calculate changes in  $E_{kf}$ , the part of the kinetic energy of the center of mass due to forward speed. Other simple procedures give  $E_p$ , the gravitational potential energy, and  $E_{kv}$ , the kinetic energy due to vertical velocity. It is apparent that the changes in potential and forward kinetic energies are almost exactly out of phase with each other in walking, so that the total energy,  $E_{tot}$ , changes only a little throughout a walking step. The opposite is true for running, where changes in potential and forward kinetic energies are substantially in phase, leading to large changes in  $E_{tot}$  in a cycle. In Fig. 3C, an index labeled "Recovery (%)" has been plotted against speed. The recovery percentage is defined in such a way that it is 100% when the vertical energy,  $E_p + E_{kv}$ , is exactly equal in shape and amplitude to the forward energy  $E_{kf}$ , but opposite in phase. A recovery percentage of zero would mean that the vertical and forward energy curves were perfectly in phase. In walking at normal speeds, around 5 km/hr, the total mechanical energy of the body is approximately conserved, so that the "recovery" of energy between its vertical and for-

Fig 3. Force-plate records have been used to calculate changes in the mechanical energy of the center of mass of the body during walking and running. A. Walking at a normal speed, in this case 4.5 km/hr. The upper curve refers to the kinetic energy due to forward motion,  $E_{kf} = \frac{1}{2} m v_f^2$ , where  $v_f$  is the

forward speed. The middle tracing is the sum of the gravitational potential energy,  $E_p$ , and the (small) kinetic energy due to vertical velocity,  $E_{kv} = \frac{1}{2} m v_v^2$ . The bottom trace shows total energy,  $E_{tot} = E_{kf} + E_p + E_{kv}$ . Arrows show the time of heel-strike (solid line) and toe-off of the oppo-

site foot (broken line). B. Running at 5.5 km/hr and 11.9 km/hr. Unlike walking,  $E_{tot}$  goes through large changes. C. "Recovery" of mechanical energy in walking (open symbols) and running (closed symbols). Here,  $W_f$  is the sum of the positive increments of the curve  $E_{kf}$  in one step,  $W_v$  is

the sum of the positive increments of  $E_p$ , and  $W_{ext}$  is the sum of the positive increments of  $E_{tot}$  (increments a plus b in part A). In this figure, an increment is defined as the change from a local minimum to a local maximum (From Cavagna, Thys, and Zamboni 1976.)



ward forms reaches 65%. In running, this recovery falls to nearly nil. Note that changes in energy stored in an elastic form, if any, cannot be measured by a force plate alone, and are not included in any of the above

These facts will underpin everything—both experimental and theoretical considerations—yet to come in this paper. Although originally established for human locomotion, these same conclusions apply to walking and running birds, and to quadrupedal animals as well (Cavagna, Heglund, and Taylor 1977)

#### 4. Determinants of Gait

There is no unique way to describe the motions of the limbs during walking, but one description, given in 1953 by Saunders, Inman, and Eberhart, is useful because of its simplicity and its completeness. In this description, six determinants of normal gait are distinguished. Each determinant generally depends on a single degree of freedom in one of the joints.

1. Compass gait. In Fig. 4, the only motions of the lower extremities permitted are flexions and extensions of the hips. The pelvis moves through a series of arcs, where the radius of the

arc is determined by the leg length. This is called compass gait

2. Pelvic rotation. The next stage of complexity, shown in Fig. 5, allows rotary motion of the pelvis about a vertical axis. The amplitude of this motion is about  $\pm 3^\circ$  in walking at normal speeds, but increases at high speeds (Saunders, Inman, and Eberhart 1953). The effectively greater length of the leg when pelvic rotation is utilized is responsible for a longer step length

Fig. 4. Compass gait. The stance leg remains stiff at all times, and the trunk moves in an arc with each step (From Inman, Ralston, and Todd [1981]. Originally published in slightly different form in Saunders, Inman, and Eberhart [1953])

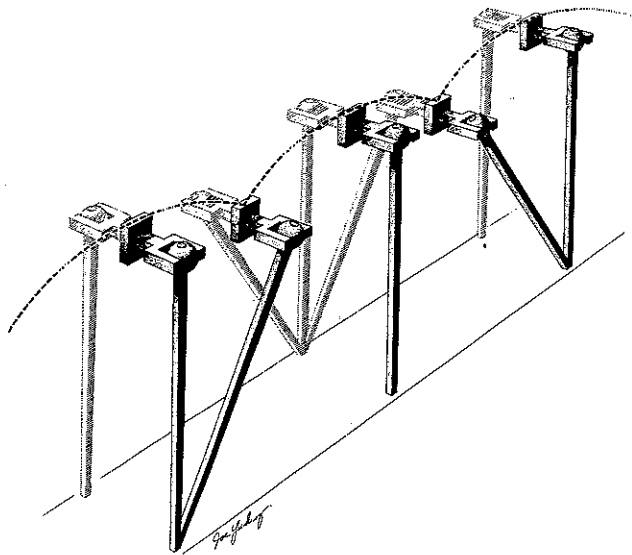


Fig. 5. In pelvic rotation, the pelvis turns about a vertical axis, lengthening the step and flattening the arcs by increasing the effective length of the leg (From Inman, Ralston, and Todd [1981]. Originally published in slightly different form in Saunders, Inman, and Eberhart [1953])

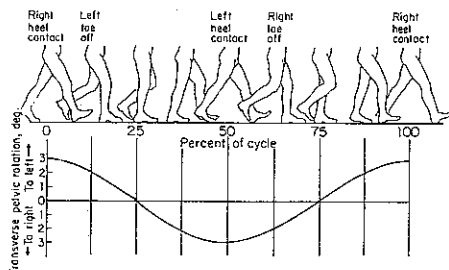
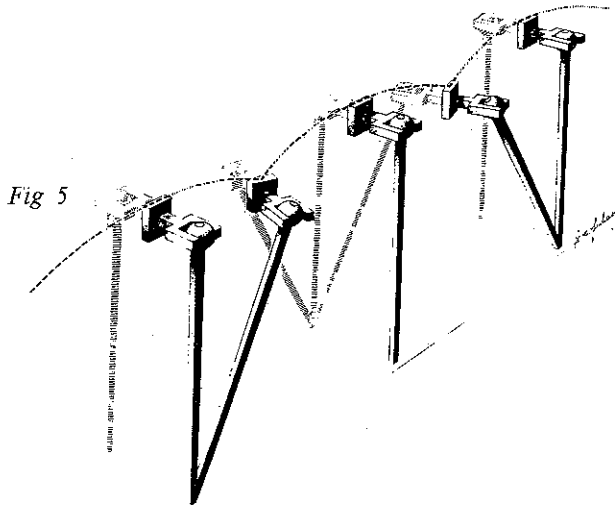
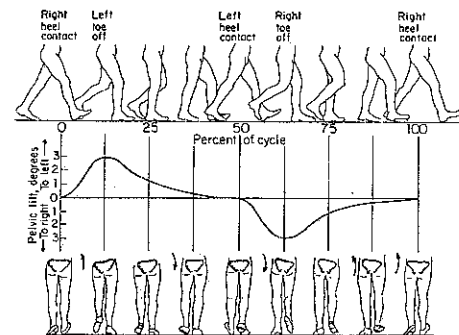
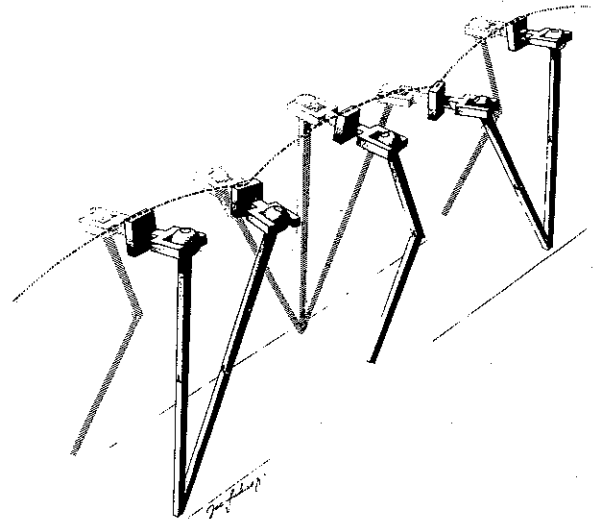


Fig 6 Adding pelvic tilt to pelvic rotation flattens the arcs further. Just before toe-off, the pelvis is lowered abruptly on the swing-leg side, then raised slowly until

heel-strike (From Inman, Ralston, and Todd [1981]. Originally published in slightly different form in Saunders, Inman, and Eberhart [1953])



and a greater radius for the arcs of the hip, hence a smoother ride. Walking racers use a walking style that depends on exaggerated pelvic rotation. In this way, they are able to delay the transition from walking to running yet maintain high speeds.

3. Pelvic tilt. When the pelvis is allowed to tilt, so that the hip on the swing side falls lower than the hip on the stance side, the arcs specifying the trajectory of the center of the pelvis are made still flatter. As shown in Fig. 6, the lowering of the swing hip occurs rather abruptly at the end of the double-support phase, just before toe-off of the swing leg. The swing hip then rises slowly through the remainder of the swing period. Note that the introduction of this determinant necessarily also brings in the requirement for knee flexion of the swing leg.

Fig 7 Knee flexion of the stance leg is added to pelvic rotation and pelvic tilt. (From Inman, Ralston, and Todd [1981]. Originally published in slightly different form in Saunders, Inman, and Eberhart [1953].)

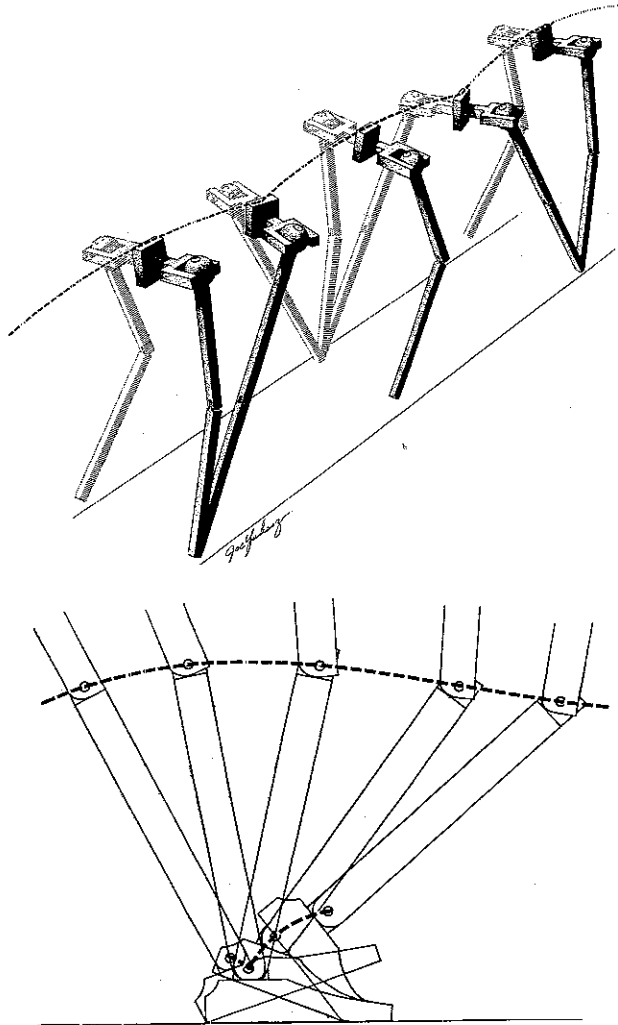


Fig 8

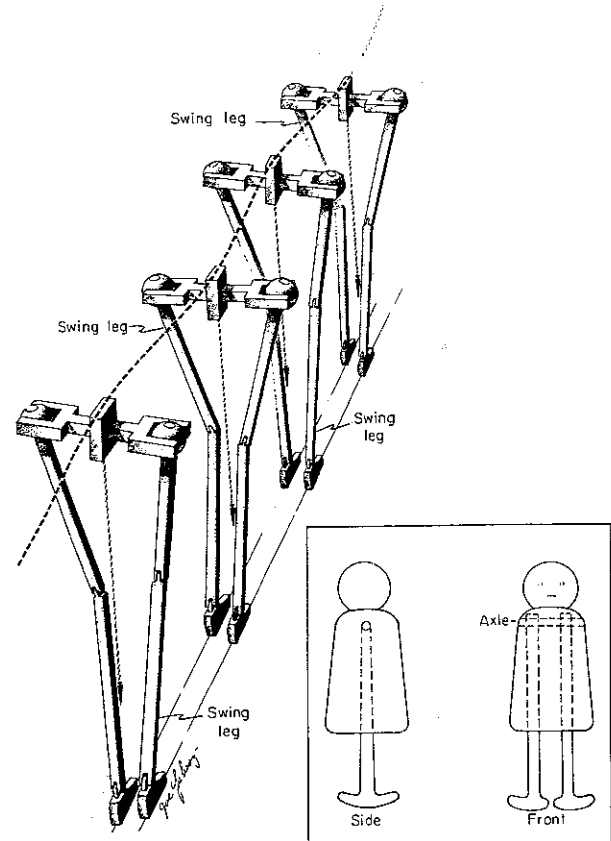
Otherwise, with the swing hip lower than the stance hip, the foot of the swing leg would strike the ground as it moved forward.

4. Stance-leg knee flexion. In Fig. 7, flexion of the stance leg has been added to the determinants listed so far (Figs. 1-6). The effect has been to flatten further the arcs traced out by the center of the pelvis.
5. Plantar flexion of the stance ankle. To smooth the transition from the double-support phase to the swing phase, the ankle of the stance leg

Fig. 8 Ankle plantar flexion of the stance leg is added to knee flexion. Most of the plantar flexion occurs just before toe-off. (From Inman, Ralston, and Todd [1981]. Originally published in slightly different form in Saunders, Inman, and Eberhart [1953].)

Fig. 9. Lateral displacement of the pelvis, a sinusoidal motion at half the frequency of the up-and-down motions. Inset Walking toy, which moves down shallow inclines by a complex motion that includes lateral rocking and pendular swinging of the

legs. The legs are fastened to the body by an axle, as shown. (Illustration of lateral displacement of the pelvis from Inman, Ralston, and Todd [1981]. Originally published in slightly different form in Saunders, Inman, and Eberhart [1953].)



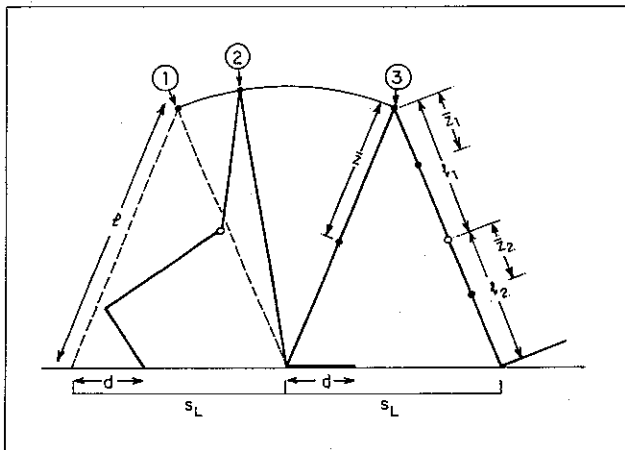
plantar flexes (sole, or plantar surface of the foot, moves down) just before toe-off (Fig. 8). Plantar flexion also plays an important part in establishing the initial velocities of the shank and thigh for the subsequent swinging motion.

6. Lateral displacement of the pelvis. Because weight bearing is transferred alternately from one limb to the other and because there is a finite lateral separation between the lower limbs, the body rocks from side to side somewhat during walking. The frequency of this lateral motion is half the frequency of the vertical excursions of the pelvis (Fig. 9).

The bipedal toy shown in Fig. 9 (inset) walks down shallow grades by making lateral rocking motions synchronized with the swinging of its pendulum legs. As the toy rocks to the left, the right leg is free to swing forward, and therefore it arrives in the correct

Fig 10. Ballistic walking model with stiff stance leg. The mass of the legs is assumed to be distributed over their length in a realistic way, so that the center of mass of the thigh is  $\bar{Z}_1$  from the hip, and the center of mass of the shank, including the foot, is  $\bar{Z}_2$  from the knee. The mass of the trunk, arms, and head is lumped at the hip. Muscles act during double support, between po-

sitions 1 and 2, to establish initial conditions on all the angles and velocities of the limbs. Thereafter, between positions 2 and 3, no muscular torques act on the swing leg, and the model moves forward under the action of gravity (and the momentum established by the initial velocities) until heel-strike (From Mochon and McMahon 1980)



position to catch the weight as the toy rolls back to the right. The energy needed to overcome friction is supplied by the fact that the toy steps down a bit with each step forward.

The frequency of the lateral motions of the walking toy is strongly amplitude-dependent. As the amplitude of the lateral rocking decreases, the frequency increases. A penny that has been spinning on a tabletop and is finally coming to rest shows this same behavior: the pitch of the sound it makes becomes higher and higher just before it lies flat. The walking toy lowers its cadence as it walks faster down steep slopes. This is just the opposite of what can be observed in human walking, where a faster speed leads to a somewhat higher stepping frequency. Nevertheless, human walking has quite a lot to do with the motions of a pendulum, as we shall see

## 5. Ballistic Walking

Electromyographic records obtained from electrodes in the leg muscles show that there is very little activity in the swing leg during walking at normal speed, ex-

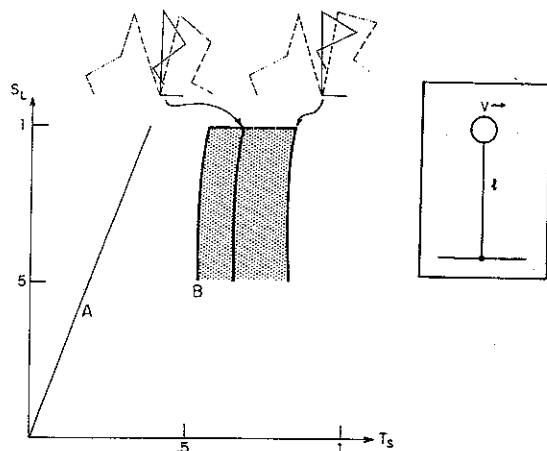
cept at the beginning and the end of the swing phase (Basmajian 1976). The muscles are active during the double-support period, when the initial conditions on the angles and velocities of each of the limb segments are being established. Thereafter, the muscles all but "turn off" and allow the leg to swing through like a jointed pendulum. A theory for walking based on these observations may be called a *ballistic walking model* because, like a projectile moving through space, such a model moves entirely under the action of gravity once it begins its swing.

### 5.1. DEFINING THE MODEL

A schematic diagram of the ballistic walking model is shown in Fig. 10. It consists of three links, one for the stance leg and one each for the thigh and shank of the swing leg. The foot of the swing leg is attached rigidly to the shank at right angles. The stance foot may be ignored, since it remains planted on the ground.

The mass of the trunk and upper part of the body is lumped at the hip joint, but the masses of the lower limb segments are distributed in a realistic way. The equations of motion for this system are derived (most conveniently, using Lagrange's equations) and programmed on a computer. Arbitrary initial conditions are chosen for the angles and velocities of the leg, thigh, and shank with respect to the vertical, subject to the condition that the toe of the swing leg must leave the ground just as the swing starts. Then the equations are solved, taking small forward increments in time, until the heel of the swing leg strikes the ground. This establishes the duration of the swing period, during which the model moves from configuration 2 to configuration 3 in Fig. 10. By trial and error, the set of initial conditions on the angular velocities of the thigh and shank is determined for each step length,  $s_L$  (for walking, step length is the distance between heel strikes). A correct choice of initial conditions just permits the swing-leg knee to come to full extension at the moment the heel strikes the ground. If the choice of initial velocities has been incorrect, the knee locks before heel strike. Another condition requires that the toe of the swing leg must not strike the ground during midswing.

Fig. 11. Calculated range (shaded area) for the normalized time of swing,  $T_s$ , as a function of normalized step length,  $S_L$ , for the model of Fig. 10. The stick figures show the moment of toe-off (broken lines, left), maximum knee flexion (solid lines), and maximum hip flexion (broken lines, right) for a normalized step length,  $S_L = s_L/\ell = 1.0$  and a maximum knee flexion of  $90^\circ$  (left diagram) and  $125^\circ$  (right diagram). To the left of curve B, the toe of the swing leg strikes the ground. To the left of line A, the model flies off the ground at midstance. Inset: An inverted pendulum of length  $\ell$  pulls upward on its pivot when  $v^2 \geq g\ell$ . (From Mochon and McMahon 1980)



## 5.2 RESULTS OF THE BALLISTIC MODEL

The condition that the toe of the swing leg not strike the ground during midswing turns out to be very important in determining the kinematics of ballistic walking. In Fig. 11, the calculated range of times of swing  $T_s$  is shown as a function of the normalized step length,  $S_L = s_L/\ell$ , where  $\ell$  is the leg length. Here  $T_s = T/T_n$ , where  $T$  is the swing time in seconds and  $T_n$  is the natural half-period of the leg as a rigid pendulum,  $T_n = \pi(I/mg\bar{Z})^{1/2}$ , with  $I$  the moment of inertia of the rigid leg about the hip, and  $\bar{Z}$  the distance of the leg's center of mass from the hip. For a leg length of 1.0 m,  $T_n$  is approximately 0.82 s.

The line B in Fig. 11 indicates the boundary between those steps (to the left of the line) in which the toe of the swing leg strikes the ground during some intermediate phase of the swing period, and those steps (to the right) in which it clears the ground. By comparison, the line A in the figure shows the boundary determined by the requirement that the vertical force shall always remain positive. Combinations of  $S_L$  and  $T_s$  to the left of line A correspond to a swing phase so rapid that the model flies off the ground. An inverted pendulum has this same behavior: its weight will be negative when

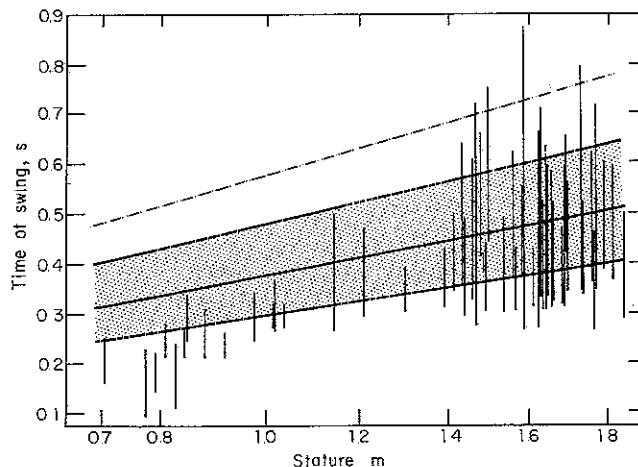
$v^2/g\ell \geq 1.0$ , where  $v$  is the velocity of the pendulum at the top of its swing (inset, Fig. 11). The point is that line B lies to the right of line A, and therefore constitutes the minimum-swing-time boundary for ballistic walking. For a given step length, as  $T_s$  is reduced, the model will begin stubbing its toe long before it flies off the ground.

A short explanation of the other boundaries of the shaded area in Fig. 11 is in order. In the case where the normalized step length  $S_L = 1.0$ , the stick figures at the top of the diagram show the model at the instant when the toe leaves the ground (broken lines, left), when maximum knee flexion occurs (solid lines), and at the moment of maximum hip flexion (broken lines, right). The stick figure on the left shows a maximum knee flexion of  $90^\circ$ . The near-vertical solid line extending below the arrow defines the locus of points where maximum knee flexion is always  $90^\circ$ . If the initial knee-flexion velocity is made greater, the time of swing is prolonged, and the knee-flexion angle reaches a greater maximum. The stick figure on the right shows a maximum knee flexion of  $125^\circ$ . The entire right-hand border of the shaded area represents ballistic steps in which knee flexion has reached  $125^\circ$  (taken to be a physiological limit) at some point during the swing. As mentioned earlier, for the solution to be accepted, the knee always comes to full extension just at the moment of heel strike.

The predictions of the ballistic walking model are compared with experimental observations in Fig. 12. In the experiments, subjects of different heights (stature) were asked only to walk at a range of different speeds, from their slowest to their fastest comfortable walking speed (Grieve and Gear 1966). The range of swing times, measured in fractions of a second, was recorded using a photographic technique. The range for each subject is shown as a vertical bar. The broken line shows the swing time (half-period) of a passive compound pendulum, where the knee is assumed to be a free joint and the mass is assumed to be distributed in a realistic way, as it was for the ballistic model. The conclusion must be that the range of swing times is confined to periods much shorter than the free period of the leg alone, acting as a pendulum. We shall return to this point later.

Also shown in Fig. 12 is a shaded range corresponding to the ballistic walking predictions. The lower

Fig. 12 Time of swing against stature. Vertical lines show experimental ranges adopted by subjects of different heights walking at a range of speeds. The broken line, which has a swing time too long to agree with the experimental range, was calculated from the half-period



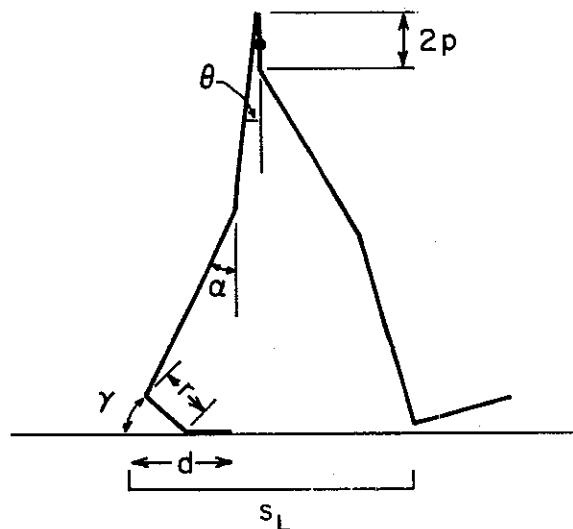
boundary of the shaded region corresponds to the limit where the toe just clears the ground during the swing. The upper boundary corresponds to the  $125^\circ$  maximum-knee-flexion line in Fig. 11. The shaded region encompasses most of the times of swing observed experimentally, with the exception of those subjects less than about 1.2 m in height, all of whom were young children. Workers investigating gaits have often remarked that young children walk differently from adults. Evidence from Fig. 12 shows that young children could make better use of gravity while walking if they cared to use longer times of swing.

### 5.3 EXTENSIONS TO INCLUDE ADDITIONAL GAIT DETERMINANTS

The ballistic walking model may be extended to include, one by one, the additional gait determinants of knee flexion of the stance leg, plantar flexion of the stance ankle, and pelvic tilt (Mochon and McMahon 1981). One may imagine gear- or cam-driven mechanisms that impose realistic functional relationships between the angles  $\gamma$ ,  $\alpha$ , and  $\theta$ , and between  $\theta$  and the length  $2p$  of the vertical component of the pelvic link, shown in Fig. 13. In this way, all the links of the stance leg go through a characteristic motion that depends on only one angle, knee angle  $\alpha$ . Given  $\alpha$ , the

Fig. 13 Extension of the ballistic walking model to include knee flexion of the stance leg ( $\alpha$ ), plantar flexion of the stance ankle ( $\gamma$ ), and pelvic tilt (through the additional pelvic link). The stance foot, whose total

length is  $d$ , now has a hinge at distance  $r$  from the ankle. Angles  $\alpha$  and  $\theta$  are defined with respect to the vertical. A coupling is assumed to exist between  $\alpha$  and each of the parameters  $\gamma$ ,  $\theta$ , and  $p$ .



stick figure is completely determined from the ground to the hip joint of the swing leg, because  $\gamma$ ,  $\theta$ , and  $2p$  are automatically determined by the various hypothetical gear or cam drives. The hip and knee of the swing leg continue to move freely under gravity with no muscular torques, as before.

The mechanical couplings do not add to or subtract from the total energy of the body during the swing. They simply act as guides for the motion of the swing hip, the way a frictionless roller coaster is guided by its track.

It turns out that the conclusions of the original ballistic walking model (Fig. 10) are changed very little by the additional gait determinants of Fig. 13, at least with respect to ranges of swing time versus step length, swing time versus stature, and so on. The one important change comes in the vertical force. The original ballistic walking model came close to predicting the correct amplitude and shape of the fore-and-aft horizontal force, but it made a poor prediction of the vertical force (in comparison with an experimental force-plate record). The introduction of a realistic form for stance-leg knee flexion and extension did little to improve the shape of the vertical force, which still dropped to unrealistically low values toward the end of the swing. Only with the addition of pelvic tilt (giving a vertical force rise at the beginning of the swing phase) and stance-leg plantar flexion (giving a force



rise toward the end of the swing) did the vertical force predicted from the model conform with a typical measured force record

#### 5.4. CONCLUSIONS FROM BALLISTIC WALKING STUDIES

Recall that the motivation for the ballistic walking model was the observation of Fig. 3A that the sum of the kinetic plus potential energies of the center of mass of the body changed relatively little during the swing phase of a walking step. This observation was used as a basis for the ballistic walking model in both its original and extended forms.

A central conclusion from the analysis was that the half-period of the swing leg alone, represented as a jointed pendulum hanging from a fixed support, was much longer than the experimentally observed range of times of swing (Fig. 12), but the range predicted by the original ballistic walking model (Fig. 10) was in reasonable agreement with experimental data. Apparently, then, the coupling between the stance leg (acting as an inverted pendulum) and the swing leg (acting as a compound pendulum) is very important in determining the dynamics of normal walking.

Therefore, our first conclusion will be that the model of Fig. 10 is the least complicated mechanical configuration one ought to have in mind when thinking about the dynamics of walking. A compound pendulum alone or an inverted pendulum alone is not enough.

The second conclusion has to do with the role of the various determinants of gait in walking dynamics. According to the model of Fig. 13, the additions of stance-leg knee flexion, stance-leg ankle plantar flexion, and pelvic tilt do not make dramatic changes in the swing period, but the last two are necessary to obtain agreement between the predicted and observed vertical ground-reaction forces. This confirms the remark often made about the function of the calf muscles during walking—that they act to smooth the transitions between the arcs of compass gait. It does not detract, however, from the one central lesson of the ballistic walking story.

That lesson is that the action of gravity is so important in determining the dynamics of walking that a model (Fig. 10) that includes no muscular torques at

all during the swing phase can give a satisfactory representation of human walking at normal speeds.

In spite of this success, the ballistic walking model has its limitations, which must be recognized. It does not acknowledge a significant role for the arms and trunk in walking dynamics, although they may well have one. It is confined to the sagittal plane, and therefore does not consider the kind of coupling between lateral rocking motions and forward swinging motions that allowed the walking toy of Fig. 9 to work and that may be an important feature of human walking at low speeds. Finally, the assumption of zero muscular torques at the joints of the swing leg makes the model unable to represent walking at very low or high speeds, or running.

#### 6. Locomotion in Reduced Gravity

Because walking at normal speeds involves a rhythmic exchange between kinetic and potential energy, walking under conditions of reduced gravity (e.g., on the moon) has to be confined to a lower range of walking speeds. This is because the changes in potential energy that can be stored against gravity are reduced, and hence the changes in kinetic energy of the center of mass must be reduced, when gravity is reduced.

This can be seen more clearly in the context of the ballistic walking model. In Fig. 11, the line B shows the minimum normalized time of swing required for the leg to clear the ground. For any particular step length,  $T_s$  will be given by a point on this line: for example, when  $S_L = 1.0$ ,  $T_s = 0.55$ . Since  $T_s$  is expressed as a normalized time, the actual number of seconds,  $T$ , required for the swing will change as gravity changes. In fact, since the moon's gravity is only one-sixth that of the earth,

$$\frac{T_{\text{moon}}}{T_{\text{earth}}} = \frac{T_{n,\text{moon}}}{T_{n,\text{earth}}} = \sqrt{6} = 2.45, \quad (1a)$$

where

$$T_n = \pi (I/mg\bar{Z})^{1/2} \quad (1b)$$

is the half-period of a pendulum representing the leg with the knee locked, as defined earlier.

Therefore, in order for the ballistic walking model to duplicate the same trajectory of motion on the moon that it uses on the earth, the time of swing must rise by a factor of almost 2.5. As on earth, if it tries to move faster than this, it stubs its toe (or it has to give up the ballistic principle and use muscles during the swing). This means that the walking speed, for a given step length, can be only about 40% on the moon what it is on the earth.

Instead of being content with such a severe restriction of speed, when the Apollo astronauts were on the moon, they preferred to move about in a series of jumps a few centimeters in height. They could have jumped higher and therefore moved faster if they had wanted to. Margaria and Cavagna (1972) have calculated that the height of a maximal jump on the moon would be about 4 m.

## 7. Elastic Storage of Energy

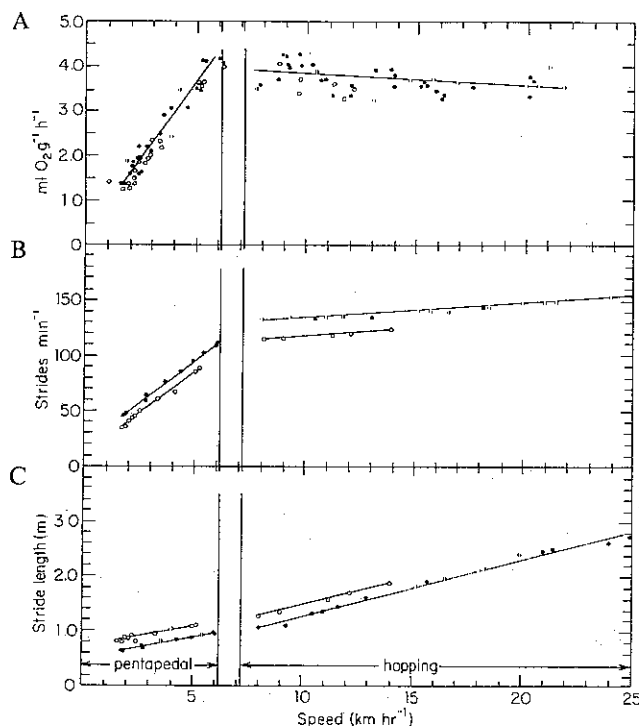
Recall from Fig 3B how very different the fluctuations in potential and kinetic energy are for running, as opposed to walking. For running, both gravitational potential energy,  $E_p$ , and forward kinetic energy,  $E_{kf}$ , reach a minimum in the middle of the support phase, and both go through a maximum as the body takes off and flies through the air. The fact that the total energy,  $E_{tot} = E_{kf} + E_p + E_{kv}$ , goes through large fluctuations during the time the feet are on the ground shows that mechanisms of the pendulum type for conserving total energy are not very important in running.

### 7.1. ENERGETICS OF KANGAROOS

What is important in running, however, is the storage of energy in an elastic form, as opposed to a gravitational form. A clue to this is found in the study of the energetics of kangaroos (Dawson and Taylor 1973).

At low speeds, kangaroos move in a mode of progression that has been called "pentapedal," since the animal uses all four limbs and the tail. A gait cycle starts with the hind feet and the tail on the ground. The animal lowers the front feet to the ground, pulling the tail toward the body, and swings the hind limbs forward. It then lifts the front feet and moves them

forward, repeating the cycle. At a speed between 6 and 7 km/hr, kangaroos change to the hopping mode, which involves only the hind limbs moving in synchrony.



hopping begins. C. Speed increases are achieved primarily by increases in stride length during hopping. Points represent data from two females weighing 18 kg (solid circles) and 28 kg (open circles) (From Dawson and Taylor 1973)

forward, repeating the cycle. At a speed between 6 and 7 km/hr, kangaroos change to the hopping mode, which involves only the hind limbs moving in synchrony.

In the experiments whose results are shown in Fig. 14, kangaroos wore a lightweight ventilated face mask while hopping on a treadmill. In all the experiments, the rate of working was kept below the maximal aerobic rate. This was known because the repayment of oxygen debt after a run was never more than 2% of the oxygen consumed during a run.

Not surprisingly, the rate of oxygen consumption increased sharply with speed during pentapedal locomotion. When the animals began to hop, however, the rate of oxygen consumption *decreased* with increasing speed, reaching a very flat minimum around 18 km/hr, before increasing slightly at higher speeds. The frequency of the hopping motion changed very little, although the speed changed from 8 to 25 km/hr. This, of course, meant that the animals achieved speed increases primarily by increasing stride length during hopping.

Kangaroos have large Achilles tendons. In the 40-kg animal Dawson and Taylor (1973) dissected, the Achilles tendon was 1.5 cm in diameter and 35 cm in length. It seems plausible that substantial quantities of elastic energy might be stored in the tendons immediately following the animal's impact with the ground, to be released later as the animal rebounds into the air. Broad sheets of tendon running along the ventrolateral and dorsolateral aspects of the tail may also have a role in the transient storage of elastic energy, since the tail is very heavy.

## 7.2. MAINTAINING A RESONANT SYSTEM IN MOTION

An experiment that may be considered analogous to some features of kangaroo hopping is shown in Fig. 15A. A subject grasps a handle with both hands. The handle is connected to a 20-lb weight via a spring. The weight slides on a vertical guide rod (not shown). By jiggling the handle up and down, the subject causes the weight to move up and down with amplitude  $A$ . The subject synchronizes the motions with the beat of a metronome. A pen recorder displays the amplitude,  $A$ , continuously so that the subject may keep it fixed at a prescribed level. The energy cost of making this motion is recorded by monitoring the subject's oxygen consumption with a lightweight ventilated face mask.

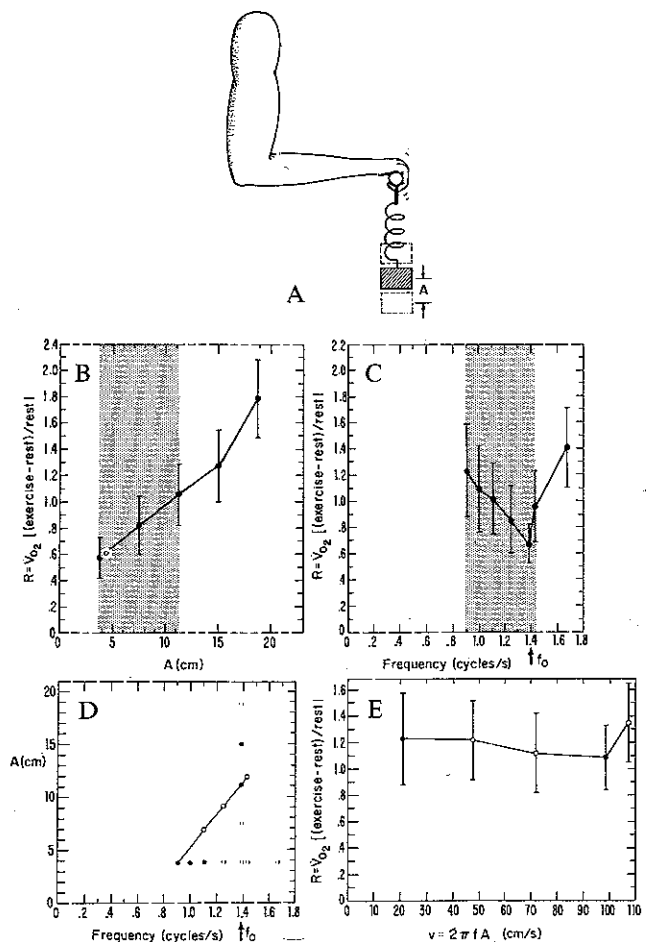
When the frequency of the jiggle motion is fixed at any one value,  $f$ , increases in the amplitude of the motion of the weight are accompanied by proportional increases in the amplitude of the periodic force felt at the hand, since the spring is linear. The increased force amplitude leads to an increased rate of oxygen consumption, as shown in Fig. 15B.

Suppose instead that the subject keeps  $A$  fixed while slowly increasing  $f$ . In this case, the amplitude of the handle motions and therefore the effort required drops to a minimum at the (damped) natural frequency of the mass-spring system,  $f_0$  (Fig. 15C). In these experiments,  $f_0$  was determined independently by observing the "ringing" frequency of the weight with the handle fixed.

The rate of oxygen consumption therefore is a function of both  $f$  and  $A$ . These experiments, involving five young adult male subjects who had first trained on this exercise for two weeks, were conducted at five

Fig. 15. Experiment analogous to kangaroo hopping. A. A handle connected to a spring supporting a weight is grasped with two hands and shaken at frequency  $f$ . The amplitude of the motion of the weight is  $A$ . B. When  $f$  is fixed, the force at the hand rises directly with amplitude  $A$ , causing the rate of oxygen consumption to rise monotonically with  $A$ . C. If the subject moves the hands so as to keep the amplitude  $A$  fixed, the effort required goes through a minimum at the (damped) natural frequency of the mass and spring,  $f_0$ . D. The experiments were conducted at five amplitudes for one frequency and at seven frequencies for one amplitude (solid points). Using the results, one may

interpolate additional points (open circles) from  $R = R_0 + (\partial R / \partial f) \Delta f + (\partial R / \partial A) \Delta A$ , where  $R$  is the increase in the rate of oxygen consumption above resting level divided by the resting level,  $R = [(exercise-rest)/rest]$ , and  $R_0$  is a value of  $R$  measured in the experiment. E. When  $A$  and  $f$  are increased simultaneously through the shaded ranges in B and C,  $R$  first falls then rises with the maximum speed  $v = 2\pi f A$ . This behavior is similar to that shown in Fig. 14A. The bars about each point show one standard deviation from the mean. (Data on five male subjects, aged 19–22, are from unpublished experiments by P. Cayer and T. A. McMahon.)



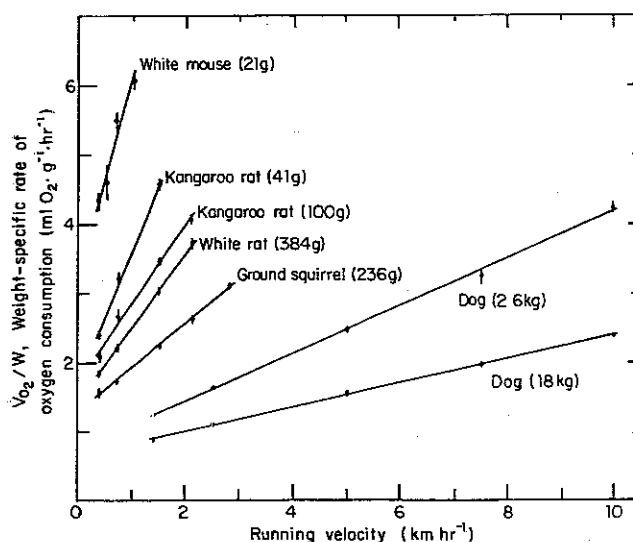
amplitudes for a single frequency and at seven frequencies for a single amplitude (solid points in Fig. 15D). Assuming that the surface determining the rate of oxygen consumption as a function of  $f$  and  $A$  is reasonably smooth, one may use those results to interpolate points along a line like the one shown in Fig. 15D, where both  $A$  and  $f$  are increasing simultaneously in a series of steps through the ranges shown shaded in parts B and C of the figure. The results, plotted in part E, show that the rate of oxygen consumption falls slowly to a minimum and then rises again, when plotted against the maximum speed of the weight,  $v = 2\pi fA$ . This behavior is essentially similar to the observed dependence of oxygen-consumption rate on running speed found in hopping kangaroos (Fig. 14A). The spring in the present experiments is analogous to the various energy-storage elements in the kangaroo's body, including (but not limited to) tendons in the legs and tail. The weight is analogous to the animal's body mass as it collides with the ground, and the subject's arms are analogous to the kangaroo's antigravity muscles.

Dawson and Taylor's (1973) experiments were limited by the maximum speed of their treadmill. Since kangaroos can sustain speeds of 40 km/hr, Dawson and Taylor presumably would have found a continuing increase in oxygen-consumption rate with speed if they had been able to investigate the 20–40 km/hr range.

Additional evidence in favor of the idea of elastic energy storage comes from studies where kangaroos hopped down a runway paved with a series of force plates (Cavagna, Heglund, and Taylor 1977). At a speed of 30 km/hr, it was found that the metabolic machinery was supplying (through oxygen utilization) only one-third of the power required to lift and re-accelerate the center of mass during an encounter with the ground. The other two-thirds of the energy required for each hop, plus the energy required to move the limbs relative to the center of mass, had to be accounted for by some mechanism other than aerobic muscular metabolism. This same result, with lower numbers for the conserved energy, has been shown for running men and for dogs and other animals (Cavagna, Heglund, and Taylor 1977). The conclusion follows that elastic energy must be stored transiently in stretched tendons, ligaments, muscles, and possibly

Fig. 16 Rate of oxygen consumption versus running speed. Vertical bars show  $\pm 2$  SE (standard error). Each animal shows an ap-

proximately linear increase in rate of oxygen consumption with speed. (From Taylor, Schmidt-Nielsen, and Raab 1970)



bent bones during running, very much the way energy is transiently stored in the spring of a pogo stick.

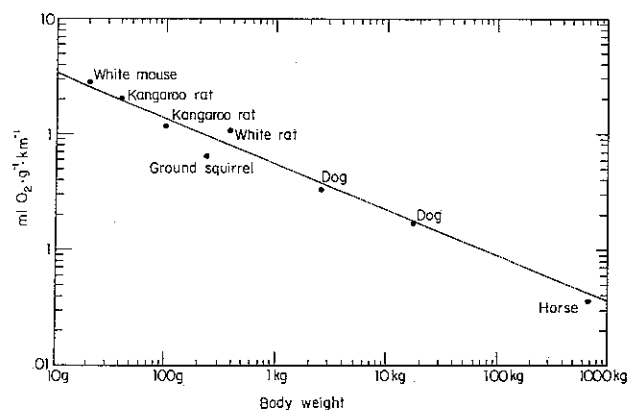
## 8. Cost of Running

A few general results have emerged that seem to describe the running energetics of animals of very diverse ancestries and body sizes. In Fig. 16, for example, the weight-specific rate of oxygen consumption is seen to be a linear function of speed for animals as different as kangaroo rats and dogs (Taylor, Schmidt-Nielsen, and Raab 1970). This same conclusion has since been shown to apply for over 50 species of animals, from pygmy mice to horses.

Suppose, for a moment, that all the lines of Fig. 16 went through the origin (they do not). Then the fact that the rate of oxygen consumption increases directly with speed would mean that the metabolic cost of moving 1 g of body weight a distance of 1 m would be a (different) constant for each animal, independent of running speed. Starting from any given reference speed, an animal might run faster, and therefore arrive where it wanted to go in less time, but the increased rate of oxygen consumption required to do so would exactly balance the reduced time, so that the same number of milliliters of oxygen would be used up in each case. The cost of running, measured in ml

Fig 17. Oxygen cost of running. Each point represents the slope of a line in Fig 16. The slope of the

solid line in this log-log plot is about  $-0.40$ . (From Taylor, Schmidt-Nielsen, and Raab 1970)



$\text{O}_2\text{g}^{-1}\text{km}^{-1}$ , therefore would be found for each animal from the slope of its line in Fig. 16.

### 8.1 COST-OF-RUNNING FORMULA

The cost of running, defined in the preceding section, was discovered to be a decreasing function of body weight. When the cost of running was plotted against body weight on log-log paper, a straight line resulted with a slope near  $-0.40$  (Fig. 17).

The fact that the lines in Fig. 16 do not go through the origin means that an intercept term has to appear in the equations describing the lines. Since the intercept term (representing the rate of oxygen consumption for running at zero speed) happens also to be a power-law function of body weight, a single formula can be given approximating all the lines in Fig. 16:

$$\dot{V}_{\text{O}_2}/W = 8.5vW^{-0.40} + 6.0W^{-0.25}, \quad (2)$$

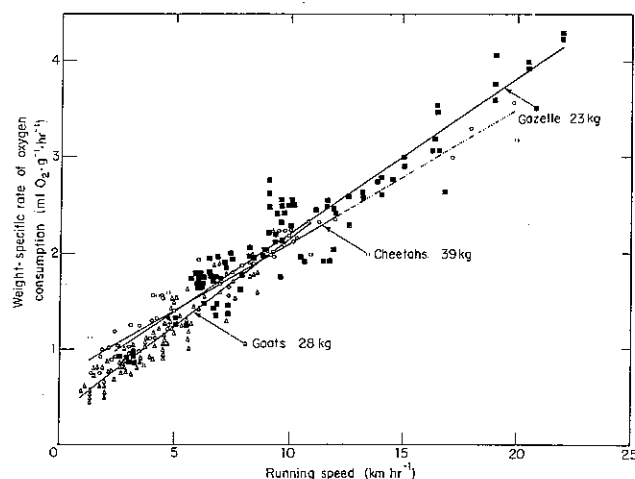
where  $\dot{V}_{\text{O}_2}$  is the oxygen consumption rate measured in ml/hr,  $v$  is the running speed in km/hr, and  $W$  is the body weight in grams.

### 8.2 INFLUENCE OF LIMBS

Before going on, it is reasonable to deal with a question having to do with the overall shape of animals. It has been assumed often by both physiologists and anatomists that a substantial part of the metabolic cost of

Fig 18. Rate of oxygen consumption versus speed for cheetahs, gazelles, and goats of comparable body weight. Although the configurations of the limbs of the animals are very different (the chee-

tah has massive limbs, the gazelle very slender ones), the oxygen cost of running at any particular speed is about the same (From Taylor et al 1974)



running should be due to overcoming the inertia of the limbs as they are accelerated and decelerated with respect to the body. If this is true, then there should be an evolutionary advantage in having the center of mass of a limb close to the shoulder or hip, decreasing the moment of inertia of the limb and thereby decreasing the metabolic cost of running at a given speed.

By way of testing this assumption, C. R. Taylor and his collaborators (1974) measured the rate of oxygen consumption of cheetahs, gazelles, and goats running on a treadmill. The animals were very similar in body weight and limb length, but the average distance to the center of mass of the limbs from their pivot points (shoulder or hip) was determined at autopsy to be 18 cm in the cheetah, 6 cm in the goat, and only 2 cm in the gazelle. Nevertheless, the rate of oxygen consumption at a given speed was almost the same in all the animals (Fig. 18).

Therefore, the work done against the inertia of the limbs probably is not a very large factor in determining the metabolic cost of running. All one needs in order to arrive at a fairly good prediction for the rate of oxygen consumption is a knowledge of the speed, the animal's body weight, and (Eq. 2). The way an animal's mass is distributed over its body and limbs appears to be of secondary importance. This is evidence in favor of the idea that the rate of oxygen consumption is determined by the extent to which the muscles maintain tension as they brake and reaccelerate the center of mass.